Optica Applicata, Vol. XI, No. 2, 1981

Numerical analysis of the imaging properties of the thermal gas lenses*

EWA SIENKIEWICZ
Institute of Physics, Technical University of Wrocław, Wybrzeże Wyspiańskiego 27, 50-370 Wrocław, Poland.

The properties of the gas lenses within the region close to the axis have been analysed by taking account of the refractive index changes depending on two variables: distance from the optical axis and the distance along the axis. The main parameters of the lens have been examined, i.e. focal distance and the shape of the principal surface. The value of the longitudinal aberration for several velocities of the gas flow and two lens lengths have been calculated and the optimal gas flow velocity found for which there exists the minimal focal length of the lens.

1. Introduction

Gas waveguides, being one of three used kinds: lens, gas, and fibre waveguides, are characterized by small losses caused by reflection and scattering of light at the air-medium boundary. Besides, they are capable of transmit ting light for long distances but suffer from considerable aberrations.

The gas lenses (as waveguide element) are classified according to thermal, hydrodynamic and electromagnetic parameters causing the variability of the refractive index in the gas medium. Because of their practical realisability and due to simple temperature dependence of the refractive index further examination should concern the thermal gas lenses with laminar gas flow working under normal atmospheric pressure, in which the air is the working medium. The gas lens used, for instance, by AOKI and SUZUKI [1] is composed of a brass tube, of constant wall temperature T_w; and a chrome-nickel wire reeled on it to heat

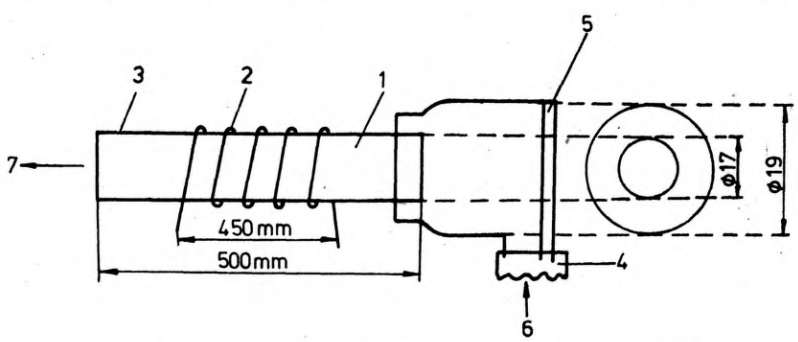

Fig. 1. Scheme of the gas lens used by AOKI and SUZUKI [1]: 1 — brass tube, 2 — copper wire, 3 — mica cover, 4 — vinyl tube, 5 — glass plate, 6 — air inlet, 7 — air outlet

* This work was carried on under the Research Project M.R. I.5.

the gas, which — being initially of room temperature T_0 — enters the tube flow through it. The air source fastened to the tube is also heated in this way. To insulate the metal tube a mica cover is applied (fig. 1). The gas heated in this way creates a radial distribution of temperature decreasing in the direction of the tube axis. This results in a corresponding refractive index gradient.

2. Ray trajectory equation

The light ray trajectory in an isotropic medium of continuous distribution of the refractive index is described by a vector ray equation [2]

$$\frac{d}{ds}\left(n\frac{d\boldsymbol{r}}{ds}\right) = \operatorname{grad} n, \tag{1}$$

where $\boldsymbol{r}$ — radius-vector of a point on the light ray,
s — length of the light ray arc,
$d\boldsymbol{r}/ds$ — unity vector normal to the wave surface,
n — refractive index of the medium.

This equation has been used by MARCUSE [3, 4]. He examined the properties of the thermal gas lens by using the paraxial approximation and assuming that the ray length change ds is approximately equal to the length change dz along the tube. He also assumed that the refractive index does not change along the lens axis, and that the medium is of angular symmetry with respect to the tube axis.

The goal of our considerations is to examine the properties of gas lenses in the off-axis region, i.e. when $ds \neq dz$ and when the refractive index changes with the length. The results will be compared with those obtained by MARCUSE [3, 4]. The ray trajectory in the gaseous medium of cylindric distribution of the refractive index may be derived easier when using the cylindric coordinate ϱ, ϱ, z system instead of the Cartesian one x, y, z. From the eq. (1) we obtain three scalar equations:

$$\begin{aligned}
&\frac{d}{ds}\left(n\frac{d\varrho}{ds}\right) - n\varrho\left(\frac{d\varphi}{ds}\right)^2 = \frac{\partial n}{\partial \varrho}, \\
&n\frac{d\varrho}{ds}\frac{d\varphi}{ds} + \frac{d}{ds}\left(n\varrho\frac{d\varphi}{ds}\right) = \frac{1}{\varrho}\frac{\partial n}{\partial \varphi}, \\
&\frac{d}{ds}\left(n\frac{dz}{ds}\right) = \frac{\partial n}{\partial z}.
\end{aligned} \tag{2}$$

By assuming that the gas medium has the rotational symmetry around the axis z, i.e. that $\partial n/\partial \varphi = 0$, the refractive index becomes a function of two variables: radius ϱ and the length z. By introducing the parametrization of the light ray trajectory and considering the light rays lying in the meridional

plane the following equation may be obtained:

$$\frac{d^2\varrho}{dz^2} = \frac{1}{n}\left[1+\left(\frac{d\varrho}{dz}\right)^2\right]\left(\frac{\partial n}{\partial \varrho} - \frac{d\varrho}{dz}\frac{\partial n}{\partial z}\right). \tag{3}$$

Since the gas lenses have great focal lengths compared to the transversal sizes of the waveguide, the value of $(d\varrho/dz)^2$ may be neglected. For gases the refractive index differs slightly from unity. This allows to write the eq. (3) in the form

$$\frac{d^2\varrho}{dz^2} = \frac{\partial n}{\partial \varrho} - \frac{d\varrho}{dz}\frac{\partial n}{\partial z}. \tag{4}$$

It has been stated experimentally that the refractive index n of the air at normal (constant) atmospheric pressure changes with the temperature T according to the formula [5, 6]

$$n(T) = 1 + \frac{0.08112}{T}. \tag{5}$$

For further examinations the temperature distribution in the thermal gas lens, given by JACOB [7] and MARCUSE [3], is accepted.

3. Temperature distribution in gas lenses

The energy balance equation in the gas lens in cylindric coordinates may be solved under following assumptions: the process is stationary, i.e. $\partial T/\partial t = 0$, the density of gas inside the tube is almost constant, the flow is laminar and viscous at constant temperature of the tube wall, the temperature field exhibits the rotational symmetry $\partial T/\partial \varphi = 0$, gravitational effect and the influence of the longitudinal thermal conductivity are neglected.

In the gas lens the following temperature distribution is obtained [3]:

$$T(\varrho, z) = T_w - (T_w - T_0)\sum_{m=0}^{\infty} A_m R_m\left(\frac{\varrho}{a}\right) e^{-\frac{a}{a^2 v_0}\beta_m^2 z}, \tag{6}$$

where T_w — tube wall temperature,
T_0 — initial temperature of the gas flowing out,
A_m — coefficient obtained from the orthonormality conditions for the eigenfunctions R_m,
$R_m\left(\frac{\varrho}{a}\right)$ — modified Whittaker functions,
a — tube radius,
β_m — eigenvalues of the function R_m,
v_0 — maximal velocity of the gas flow in the z direction,
ϱ, z — cylindric coordinates: radius and length,

$a = k/c_p \cdot \tilde{\varrho}$ — parameter characterizing the gas (k — coefficient of thermal conductivity, c_p — specific heat at constant pressure, $\tilde{\varrho}$ — average density of gas.)

By introducing the dimensionaless quantities u and x, related to the quantities ϱ and z in the following way

$$u = \varrho/a, \quad x = \frac{a}{a^2 v_0} z \tag{7}$$

a simpler form of the temperature distribution is obtained

$$T(u, x) = T_w - (T_w - T_0) \sum_{m=0}^{\infty} A_m R_m(u) e^{-\beta_m^2 x}, \tag{8}$$

and the eq. (4) takes the form

$$\frac{d^2 u}{dx^2} = \left(\frac{v_0}{V(L)} \frac{L}{a} \right)^2 \frac{\partial n}{\partial u} - \frac{du}{dx} \frac{\partial n}{\partial x}, \tag{9}$$

where $V(L) = aL/a^2$,

L — the tube length.

From eq. (9) and by virtue of (5) the following form of the differential equation of second order has been derived for the temperature distribution, mentioned above

$$\begin{aligned} \frac{d^2 u}{dx^2} = 0.08112 & \left[T_w - (T_w - T_0) \sum_{m=0}^{\infty} A_m R_m(u) e^{-\beta_m^2 x} \right]^{-2} \\ & \left\{ \frac{du}{dx} (T_w - T_0) \sum_{m=0}^{\infty} A_m R_m(u) \beta_m^2 e^{-\beta_m^2 x} \right. \\ & \left. + \left(\frac{v_0}{V(L)} \frac{L}{a} \right)^2 (T_w - T_0) \sum_{m=0}^{\infty} A_m R'_m(u) e^{-\beta_m^2 x} \right\}. \end{aligned} \tag{10}$$

The quantity $R'_m(u)$ denotes the derivative of the function $R_m(u)$ with respect to u. This equation is rather complex and should be solved numerically by using the proper programme for computer.

4. Numerical solution of the ray equation

To elaborate the computer programme the coefficients A_m and the eigenvalues of β_m calcualted by MARCUSE [4] were used and for these values the Whittaker functions $R_m(u)$ were found.

The functions $R_m(u)$ depend upon u in the following way:
– for $0 \leqslant u \leqslant 0.5$

$$R_m(u) = \sum_{n=1}^{\infty} C_n^m u^{2n-2}, \tag{11}$$

where $C_1^m = 1$,

$$C_2^m = -\frac{1}{4}\beta_m^2, \tag{12}$$

for $n \geqslant 3$, in the case when $n \geqslant 3$

$$C_n^m = \frac{\beta_m^2}{(2n-2)^2}(C_{n-2}^m - C_{n-1}^m);$$

– for $0.5 \leqslant u \leqslant 1$ it is put $w = 1-u$, and

$$R_m(w) = \sum_{k=1}^{\infty} D_k^m w^{k-1}, \tag{13}$$

where the coefficients D_k^m are expressed by the coefficients D_2^m:

$$\begin{aligned} D_1^m &= 0, \\ D_3^m &= \frac{1}{2} D_2^m, \\ D_4^m &= \frac{1}{3} D_2^m, \\ D_5^m &= \left(\frac{1}{4} - \frac{1}{6}\beta_m^2\right) D_2^m, \end{aligned} \tag{14}$$

for $k \geqslant 6$, in the case when $n \geqslant 6$

$$D_k^m = \frac{1}{(k-1)(k-2)}\left[(k-2)^2 D_{k-1}^m - \beta_m^2(2D_{k-3}^m - 3D_{k-4}^m + D_{k-5}^m)\right].$$

The functions $R_m(u)$ and their derivatives $R'_m(n)$ must be continuous at the point $u = w = 0.5$ for each m. Therefore, the coefficients D_2^m have been calculated on the basis of the above mentioned formulae, under assumption that at this point the continuity condition holds for both functions $R_m(u)$

$$D_2^m = \frac{C_1^m + C_2^m(0.5)^2 + \sum_{n=3}^{\infty} C_n^m (0.5)^{2n-2}}{0.625 + \frac{1}{3}0.125 + \sum_{k=5}^{\infty} A_k^m (0.5)^{k-1}} \tag{15a}$$

and its derivative $R'_m(u)$:

$$D_2^m = \frac{2C_2^m(0.5) + \sum_{n=3}^{\infty} (2n-2)C_n^m(0.5)^{2n-3}}{1.75 + \sum_{k=5}^{\infty} (k-1)A_k^m(0.5)^{k-2}}, \tag{15}$$

where $A_5^m = \frac{1}{4} - \frac{1}{6}\beta_m^2$,

$$A_6^m = \frac{1}{20}(16A_5^m + 2\beta_m^2),$$

$$A_7^m = \frac{1}{30}\left(25A_6^m - \frac{1}{6}\beta_m^2\right),$$

$$A_8^m = \frac{1}{42}\left[36A_7^m - \beta_m^2\left(2A_5^m - \frac{1}{2}\right)\right], \tag{16}$$

$$A_9^m = \frac{1}{56}\left[49A_8^m - \beta_m^2\left(2A_6^m - 3A_5^m + \frac{1}{3}\right)\right],$$

and for $k \geqslant 10$

$$A_k^m = \frac{1}{(k-1)(k-2)}\left[(k-2)^2 A_{k-1}^m - \beta_m^2(2A_{k-3}^m - 3A_{k-4}^m + A_{k-5}^m)\right].$$

The coefficients D_2^m, calculated according to the formulae (15a) and (15b), are practically the same only for thirteen first eigenvalues of β_m, therefore the infinite sum in (10) has been reduced to that of first thirteen terms.

For elaboration of the algorithm the summing to infinity was replaced by summing up to $n = 50$ in the case of coefficients C_n^m and to $k = 100$ for A_k^m. All the terms in series less than 0.0001 were neglected, since practically they do not influence the values of the function R_m and its derivative R'_m. In the programme the Runge-Kutty method of fourth order with the constant integration step was employed [8]. The programme of calculation of the gas lens properties has been written in the SLAM language, while the calculations were carried out on Odra 1305 computer. This programme prints the normed coordinated x and $u(x)$ of the ray for x changing by 0.02, the normed tangents of slope angles made by the light ray with the axis the points $(u(x), x)$ and normed to the lengths of z_F/L and z_H/L, corresponding to the focal length and the distance of the principal surface points, respectively. Due to a long calculation time for one sequence of data (about 15 min.) the analysis has been restricted to the lens of fixed tube diameter 2a and constant temperature difference $T_w - T_0$. The lens parameters were calculated, by taking account of more parameters in the case when the direction of the ray entering the tube and the gas flow

direction were consistent. The lens parameters were calculated only once for one gas velocity and two lengths of thew aveguide, when the directions were opposite.

5. Discussion of numerical results

On the base of differential eq. (10) a number of gas lens parameters were determined under the following initial conditions: $x = 0$, $u(x) = u_0$, and $du(x)/dx = 0$. The positions of the ray points $u(x)$ and the ray slope with respect to the tube axis $du(x)/dx$ have been found for varying parameters: distance from the axis u_0, lens length L and gas flow velocity v_0 along the tube axis. The main lens parameters, i.e. focal length and the distance of the principal surface points were calculated. The principal surface is determined by the points, which are defined by intersection of the direction of the light ray entering the lens parallelly to the lens axis with the direction of the same ray leaving the lens. The distance of the principal surface points x_H is measured from the lens origin to the point of intersection of the two ray directions. The focal length x_F is measured from the point of intersection of the principal surface and the paraxial light ray (parallel at the entrance to the lens axis) to the point of intersection of this ray with the optical axis after its leaving the lens (fig. 2).

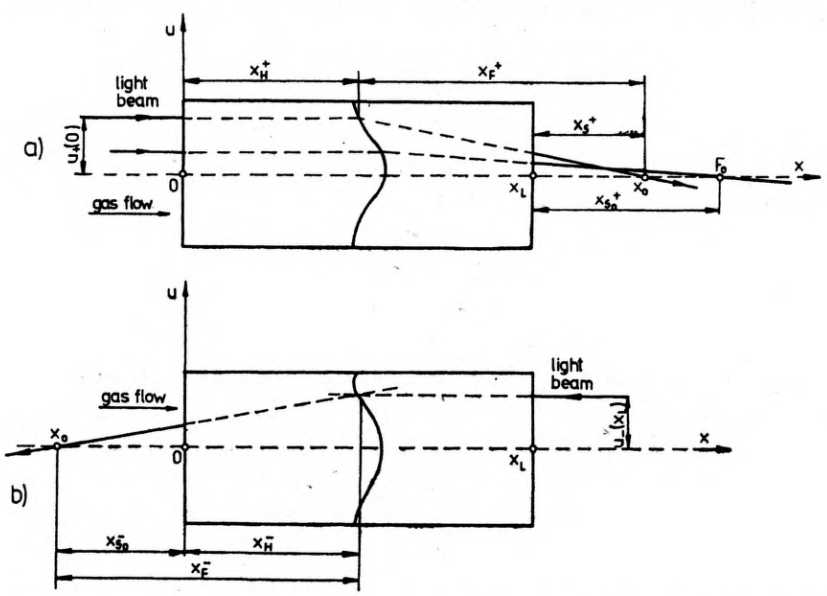

Fig. 2. Normed main parameters of the lens when the directions of the light ray and the gas flow are: a) consistent, b) opposite

Both the definitions are right in case when the direction of light ray is consistent with that of the gas flow velocity (indices "+") and also when the directions are opposite (indices "−").

The focal length and principal surface shape may be calculated from the following relations [3]:

$$\frac{z_F^+}{L} = -\frac{v_0}{V(L)} \frac{u_+(0)}{u'_+(x_L)}, \tag{17}$$

$$\frac{z_H^+}{L} = 1 + \frac{v_0}{V(L)} \frac{u_+(0) - u_+(x_L)}{u'_+(x_L)}, \tag{18}$$

$$\frac{z_F^-}{L} = \frac{v_0}{V(L)} \frac{u_-(x_L)}{u'_-(0)}, \tag{19}$$

$$\frac{z_H^-}{L} = \frac{v_0}{V(L)} \frac{u_-(x_L) - u_-(0)}{u'(0)}, \tag{20}$$

where z_F/L and z_H/L refer to the focal length and the distance of the principal surface points normed by the lens length L, respectively. Taking account of (7) the following formulae may be also used (fig. 2)

$$x_F^+ = -\frac{u_+(0)}{u'_+(x_L)}, \tag{17a}$$

$$x_H^+ = \frac{V(L)}{v_0} + \frac{u_+(0) - u_+(x_L)}{u'_+(x_L)}, \tag{18a}$$

$$x_F^- = \frac{u_-(x_L)}{u'_-(0)}, \tag{19a}$$

$$x_H^- = \frac{u_-(x_L) - u_-(0)}{u'_-(0)}. \tag{20a}$$

In all these formulae $x_L = \dfrac{a}{a^2 v_0}$, $L = \dfrac{V(L)}{v_0}$.

The calculations were made for two lens lengths $L = 20$ and 30 cm, for the following normal axial velocities of the gas flow $v_0/V(L) = 2$, 5, 6.25, 10, 20 and for ten normed distances $u(0)$ of the ray from the axis ranging from 0.1 to 1 by 0.1. In order to obtain the complete picture of the gas lens action several graphs have been drawn. All the quantities in the graph are normed, except for the lens length. The calculations are acrried out for the lens with laminar flow working at constant atmospheric pressure $p = 1014$ hPa and exploiting the air as the working medium. The temperature difference between the tube wall and the tube axis at the input is $T_w - T_0 = 50$ K, while the cylinder radius is $a = 0.3$ cm. For the laminar flow in the case of the air temperature of 293 K the maximal gas flow velocity along the tube axis is $v_{\max} = R_{cr}\mu/d\tilde{\varrho} \simeq 570$ cm/s, where R_{cr} — critical Reynolds number, μ — dynamic viscosity, d — tube diameter, $\tilde{\varrho}$ — gas density at 293 K.

The figure 3 shows the dependence of the normed focal length z_F^+/L upon the normed gas flow velocity $v_0/V(L)$ for the fixed length L of the waveguide, for rays entering the tube at the height $u(0) = 0.1$. Attempts have been made to found the focal length for the paraxial rays at the height $u(0) = 0.01$. However, the light ray incident at this height makes small angles with the optical axis and, when dividing two very small values, the computer errors cause considerable deviations of the focal length and the principal surface, compared to the respective values for $u(0) = 0.1$, which are closer to the aberrationless ones. Therefore, the plane located at the focus F_0 of the lens has been accepted

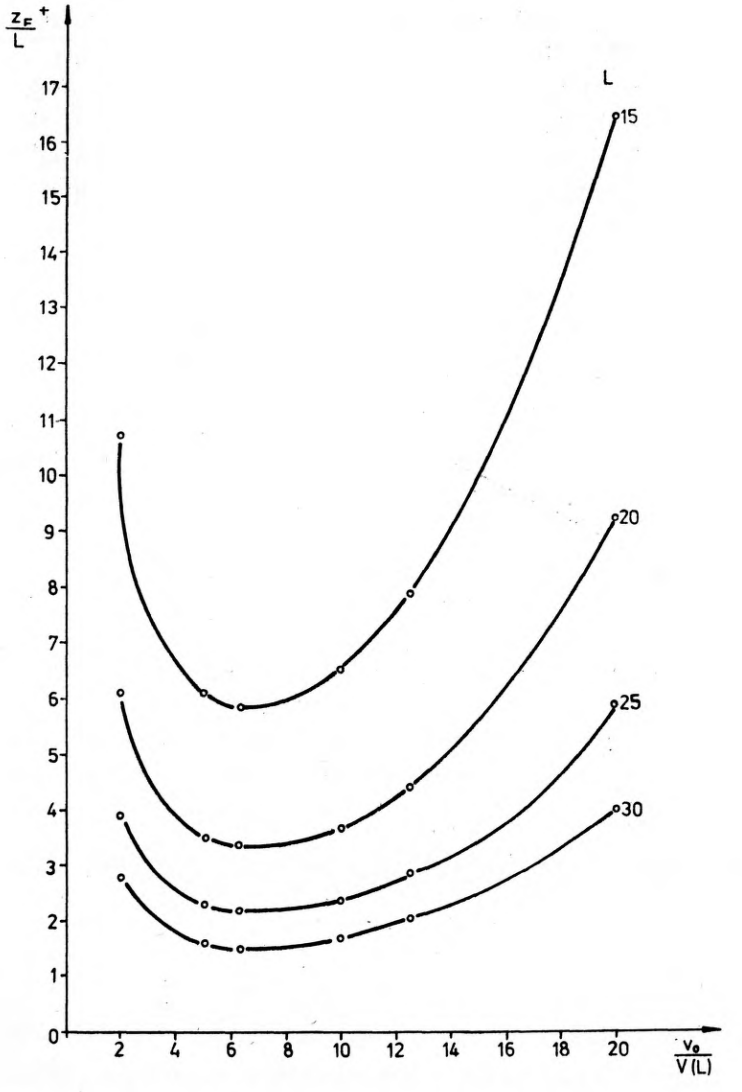

Fig. 3. The dependence of the normed focal length z_F^+/L on the normed gas velocity $v_0/V(L)$ for $u(0) = 0.1$

to be the plane of ideal imaging for the parallel rays falling on the lens at the height $u(0) = 0.1$. The graphs are made for four values of the lens length. All the curves exhibit a minimum, which corresponds to the optimal gas flow velocity v_0 for which the focal length is the least. The normed optimal velocity amounts to $v_0/(L) \simeq 6.5$. The existence of focal length minimum may be easily interpreted. For very small velocities the gas — before reaching the tube output — gets warmed to the temperature of the tube wall and the focussing action becomes very weak, while the focal lengths reach high values. An increase of the gas velocity causes that some stable temperature gradient appears, which results in increasing focussing activity of the gas and, consequently, the focal length reaches its minimum. At high gas velocities the focussing becomes weaker again, since the gas leaves quickly the tube, before its initial temperature at the lens input is changed by heating. At the fixed gas flow velocity the focal length diminishes almost inversely proportionally to the lens length with the increase of the length L. For $L = 20$ cm and $v_{\text{opt}} = 312$ cm/s the focal length is equal to $z_F = 66$ cm, while for $L = 30$ cm and $v_{\text{opt}} = 468$ cm/s it amounts to $z_F = 45$ cm.

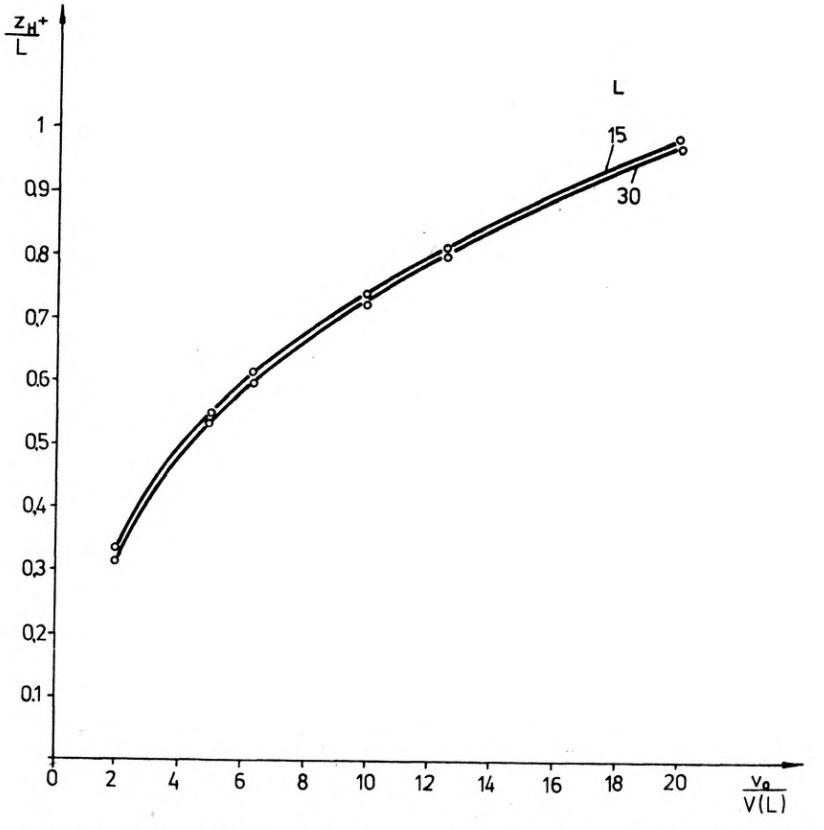

Fig. 4. Normed position of the principal surface points z_H^+/L for $u(0) = 0.1$ as a function of normed gas velocity $v_0/V(L)$

For the rays entering the lens at the height $u(0) = 0.1$, the distance of the principal surface points $z^{+}_{H/L}$ from the tube axis is presented in fig. 4 as a function of the normed gas flow velocity $v_0/V(L)$ for two values of the waveguide length L. Since the position of the principal surface points does not change practically with the lens length, therefore to clarify the graph only the points for two extreme lengths $L = 15$ cm, and $L = 30$ cm have been marked, $L = 20$ cm, and $L = 15$ cm being ignored. The difference between the distances of the principal surface points is the greatest for $v_0/V(L) = 5$, and amounts to 0.01331, which is 2% of the distance $z^{+}_{H/L}$. For small gas velocities the points of the principal surface are positioned closer to the tube origin and are shifted toward the tube inside for great values of $v_0/V(L)$.

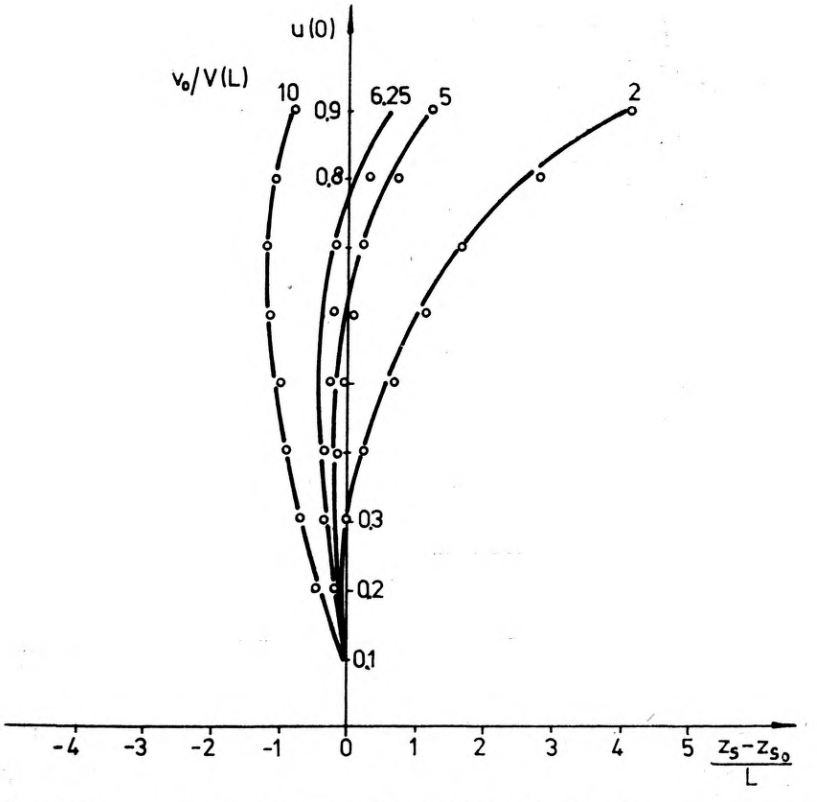

Fig. 5. The graphs of the longitudinal spherical aberration as a function of position $u(0)$ of the ray at the lens entrance for $L = 20$ cm

It has been stated that the rays parallel to the axis at various heights from the tube axis do not intersect at one point F_0 which is a paraxial image of the rays falling at the height $u(0) = 0.1$. The differences between this point and the intersection point of the real rays with the optical axis is the measure of the

longitudinal spherical aberration. For more exact aberration estimation it is more convenient to introduce the distance x_s from the lens end to the intersection point x_0 of the real ray with the tube axis (fig. 2), which may be calculated immediately from the formula

$$x_s = -\frac{u(x_L)}{u'(x_L)}. \tag{21}$$

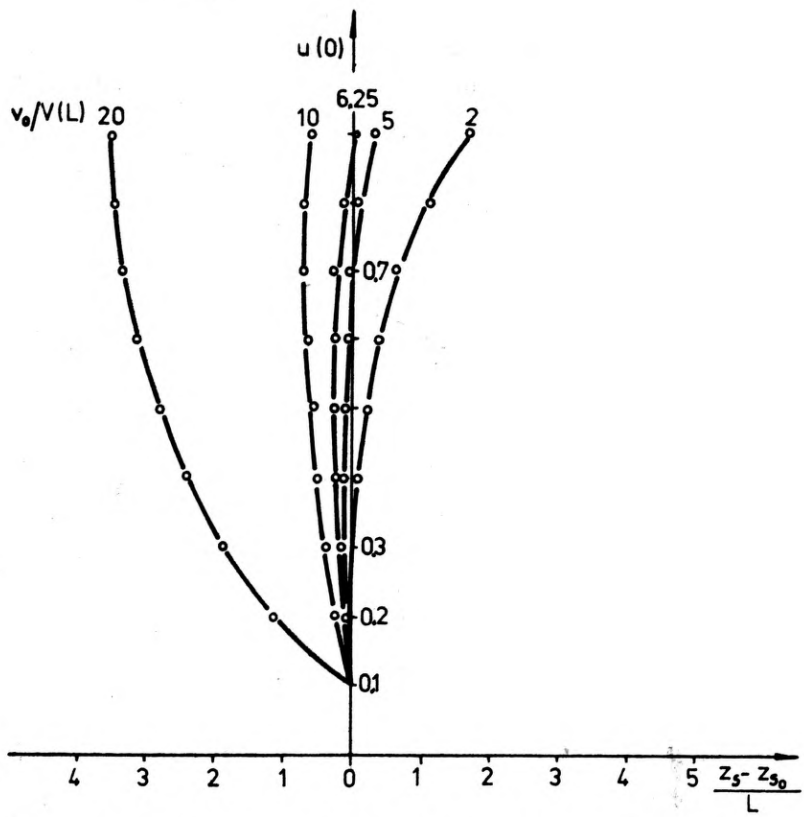

Fig. 6. The graph of the longitudinal spherical aberration as a function of the position $u(0)$ of the ray at the entrance for $L = 30$ cm

The figure 5 shows the dependence of the normed longitudinal spherical aberrations $z_s - z_{s_0} = v_0(x_s - x_{s_0})/V(L)$ on the ray position $u(0)$ at the lens entrance for several values of $v_0/V(L)$ and $L = 20$ cm. Analogical graphs for $L = 30$ cm are presented in fig. 6. Aberration decrease for gas velocities contained within the interval $5 < v_0/V(L) < 10$, and the smallest ones are in the neighbourhood of optimal velocity $v_0/V(L) \approx 6.5$ for which z_F^+/L possesses a minimum. At smaller velocities of gas flow the aberrations are rather small for the rays entering the lens closer to the tube axis. The maximal value of the aberration $(z_s - z_{s_0})/L$ for $v_0/V(L) = 6.25$, and $L = 20$ cm amounts to 0.650325 at the height $u(0) = 0.9$, which corresponds to about 13 cm, while

for $L = 30$ cm at the height $u(0) = 0.7$ $(z_s - z_{s_0})/L = 0.2370575$, which corresponds to about 7 cm. In the first case the system is overcorrected, while in the second — undercorrected. As it may be seen from the calculations the aberrations for the gas lenses are very great in comparison to those of classical lenses:

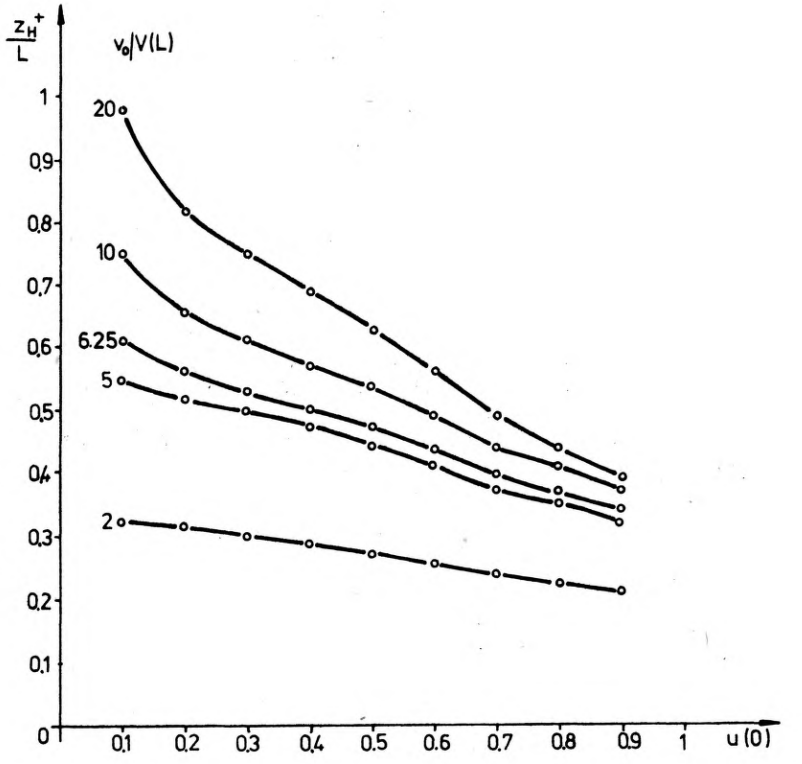

Fig. 7. The shape of the principal surface for $L = 20$ cm

The graphs in figure 7 illustrate the shape of the principal surfaces z_H^+/L at different values of $v_0/V(L)$ parameters for two waveguide length $L = 20$ cm. For the lens of the length 30 cm the shape of the principal surface is identical and, therefore, only one graph is presented. The distance of the principal surface points is calculated from the formula

$$\frac{z_H^+}{L} = 1 + \frac{z_s^+}{L} - \frac{z_F^+}{L}. \tag{22}$$

From this figure it may be seen that for different heights $u(0)$ the distance z_H^+/L changes, thus that in the gas lens the principal surfaces appear in the place of principal planes. For small velocities of the gas flow the deformation of the principal surface is the smallest, while the principal surface is positioned

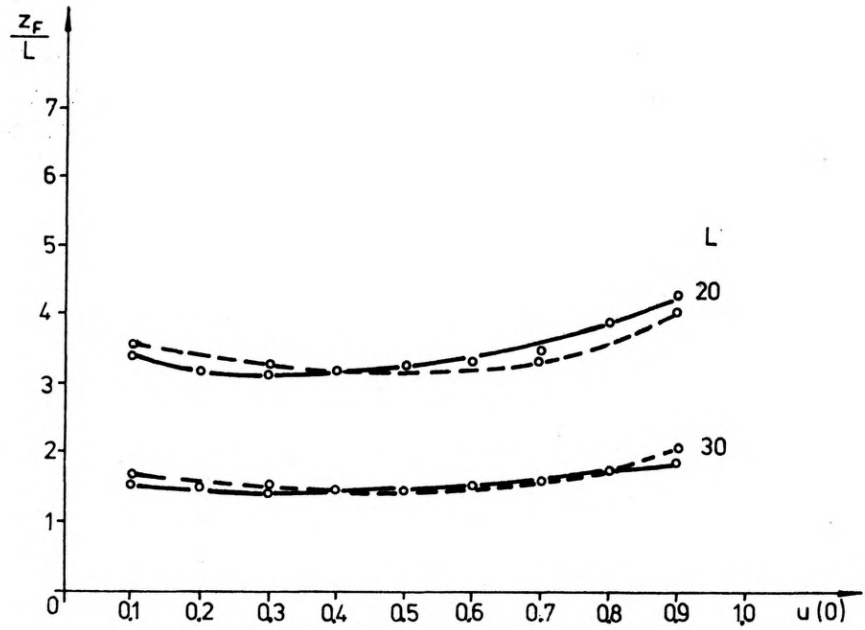

Fig. 8. Normed distance z_F/L as a function of the position $u(0)$ of the ray at the entrance for normed gas velocity $v_0(V(L) = 6.25$

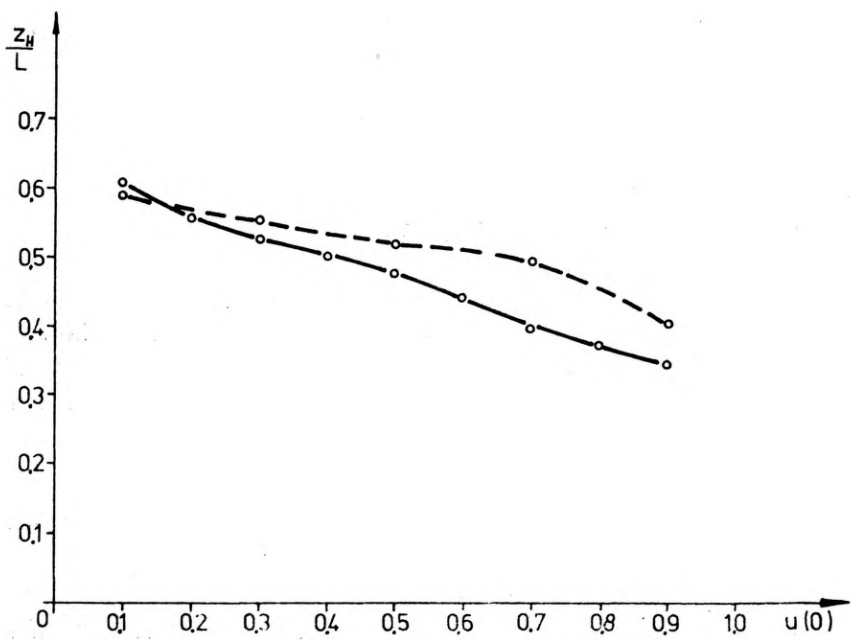

Fig. 9. The shape of the principal surface for normed gas velocity $v_0/V(L) = 6.25$ for $L = 20$ cm

closer to the lens origin. As this velocity increases the deviation from the plane increases and the principal surface is located close to the lens centre. For great velocities $v_0/V(L) > 10$ the principal surface occupies more than one third of the lens length.

The figures 8 and 9 correspond to the normed gas velocity $v_0/V(L) = 6.25$ which is close to the optimal velocity. In fig. 8 the dependence of the distance z_F/L has been presented for the cases when the light ray moves in the direction of the gas flow (continuous lines) and in the opposite direction (broken lines). In the both cases the dependences of the distance z_F/L on the position $u(0)$ of the ray at the entrance are almost identical. Fig. 9 shows the shape of the main surface for two directions of the ray run. The coverage of both the surfaces is not ideal, but the gas lens may still be treated as a thin lens.

The values calculated according to the formulae (17)–(22) are approximate, since in all the dependences there appear the tangent of the slope angle of the ray with respect to the axis at the point (u, x_L) at the end. Strictly speaking, the tangent of the ray slope with respect to the tube axis at the intersection point of (u, x_0) of the ray with the optical axis. The value of this angle varies. The gas temperature at the end of the lens is $T(u, x_L)$, and the temperature of the tube surrounding is equal to $T_0 < T(u, x_L)$. The coefficients are $n(u, x_L)$, and $n_0 > n(u, x_L)$, respectively. The ray before reaching the medium of refractive index n_0 passes through a path segment of refractive index $n(u, x_L) < n(u, x) < n_0$. Since the ray tends to bend in the direction of the medium of greater refractive index it will create greater angles with the lens axis. The increase of the ray slope angle with respect to the axis is accompanied by a decrease of the focal length z_F/L and the distance z_s/L, while the

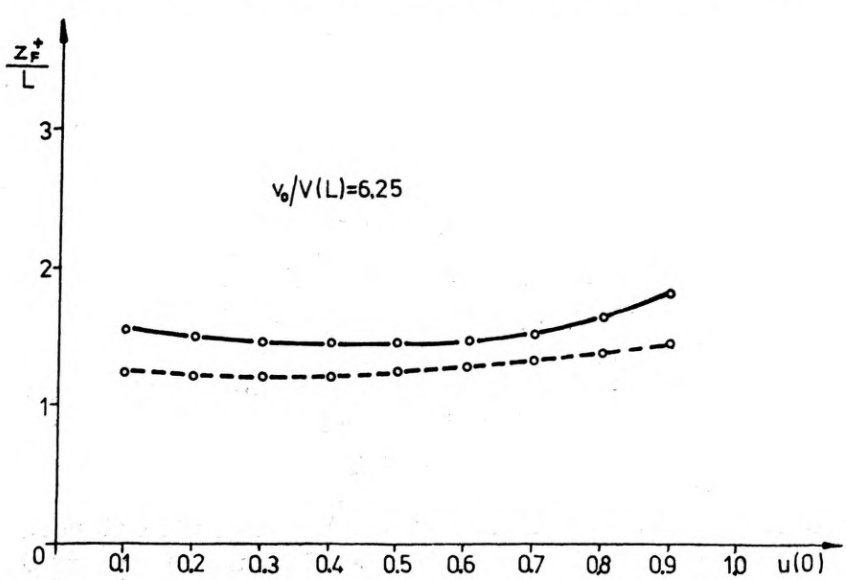

Fig. 10. Normed distance z_F^+/L as a function of position $u(0)$ of the ray at the lens entrance for $L = 30$ cm

value of z_H/L increases. In the figs. 10 and 11 the influence of the tangent of the slope angle with respect to the lens axis upon the value z_F^+/L (fig. 10) and z_H^+/L (fig. 11) are presented for the normed gas flow velocity $v_0/V(L) = 6.25$ and the lens length $L = 30$ cm. The consideration has been reduced to this single case, since the computation time of the tangent of the slope angle of the ray with the axis in the point (u, x_0) for one series of data (fixed lens length L,

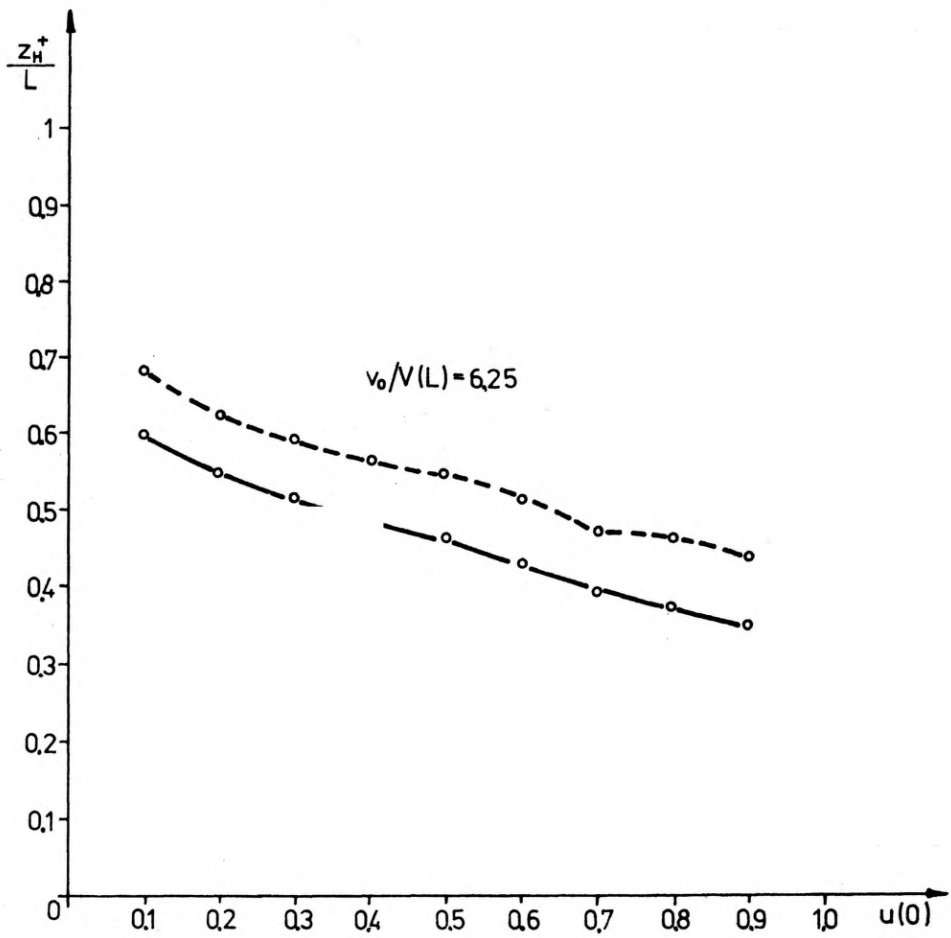

Fig. 11. The shape of the principal surface for $L = 30$ cm

gas flow velocity $v_0/V(L)$, and the ray incidence height $u(0)$) is rather great, and for small velocities ($v_0/V(L) < 6.25$) and shorter lengths may even be as high as 80 min. The solid lines refer to the values z_F^+/L and z_H^+/L representing the quantity $u'(x_L)$ in the formulae (17)–(22). The broken lines represent $u'(x_0)$. The values of the distances z_F^+/L and z_H^+/L change. The values of longitudinal spherical aberration diminish — the maximal value of aberration $(z_s - z_{s_0})/L = 0.1239$ for $u(0) = 0.7$, which corresponds to about 3.7 cm (previously about 7 cm). The principal surface is located closer to the lens centre.

6. Final remarks

The properties of the gas lens were examined in the nonparaxial region, taking account of the change in refractive system with respect to two variables: distance u from the tube axis, and the length x along the axis. The considerations were carried out for the lens in which the laminar gas flow was kept along the whole tube length and the air was treated as an ideal gas. In reality, the gas flow along the initial lens segment may be nonuniform — the velocity distribution within this segment may differ from its distributions in the further part of the lens. In practice, this part of the lens volume, in which the velocity distributions and the temperature are not yet stable, may influence the optical characteristics of the gas lens, which may be essential especially for short tube lenses [9]. However, due to the complex form of the energy balance equation in the gas lens it is assumed that the velocity distribution in an arbitrary cross-section along the whole tube length is constant.

The results of numerical calculations have confirmed that the gas medium of cylindric distribution of the refractive index may be employed to focussing of the light rays, if the temperature of the tube wall is higher than the temperature of the gas at the entrance. When analysing the results presented by MARCUSE [4] it has been stated, for example, that for the parameter $C = (n_{\text{aver}} - 1)\Delta T L^2/T_{\text{aver}} a^2 = 0.2$ corresponding to the length $L = 20$ cm, the values of the focal length z_F^+ at the highest $u(0) = 0.1$ are less than the values calculated in the nonparaxial region if the changes of refractive index along the length x of the lens are taken into account, and change for $v_0/V(L) = 6.25$ by about 7 cm, and for $v_0/V(L) = 20$ by about 30 cm. The changes in the accurate values of the distances z_H^+ of the principal surface points increase with the increase of the gas flow velocity and for $v_0/V(L) = 20$ cm they amount to about 4 cm. However, the exact quantitative analysis of the results obtained by Marcuse is impossible without tedious numerical calculations of the lens parameters according to his scheme. Besides, the parameters introduced by Marcuse corresponds rather inaccurately to the lengths $C = 15$, 20, 25, and 30 cm, for which the numerical calculations in this work have been carried out. The quantitative analysis confirms the Marcuse assumptions. The character of changes in the focal length and the shape of the principal surface for different gas flow velocities and the lens lengths are the same. The optimal gas flow velocity $v_0/V(L)$ is identical with that reported by Marcuse.

References

[1] AOKI Y., SUZUKI M., IEEE Trans. Microwave Theory Tech., **15** (1967), 2.
[2] BORN M., WOLF E., *Principles of Optics*, Pergamon Press, London 1959.
[3] MARCUSE D., *Opticheskie volnovody*, Izd. Mir, Moskva 1974.
[4] MARCUSE D., IEEE Trans. Microwave Theory Tech. **13** (1965), 734.

[5] MARTYNENKO O. G., KALESNIKOV P. M., KOLPASHCHIKOV V. L., *Vvedenie v teoriyu konvektivnych gazovych linz*, Izd. Nauka i Tekhnika, Minsk 1972.
[6] JÓŹWICKI R., *Optyka instrumentalna*, WNT, Warszawa 1970.
[7] JACOB M., *Heat Transfer*, J. Wiley and Sons, New York 1951.
[8] BERNARDYN R., *Język do modelowania układów ciągłych SLAM*
[9] KOLESNIKOV P. M., et al., Izv. AN BSSR, Ser. fiz-energ. nauk, **3** (1972), 105.

Received February 27, 1980,
in revised form, July 5, 1980,

Численный анализ отображающих свойств термических газовых линз

Проанализированы свойства газовой линзы во внеприосевой области при учёте изменения коэффициента преломления от двух переменных: расстояния от оптической оси и длины вдоль оси. Исследованы главные параметры линзы: фокусное расстояние и форму главной поверхности. Рассчитано значение продольной аберрации для нескольких скоростей течения газа и двух длин линзы, а также найдена оптимальная скорость течения газа, при которой существует минимальное фокусное расстояние линзы.